

# **The Polarization Azimuth Angle in Daylight Scenes**

Roy M. Matchko and Grant R. Gerhart

Battelle Scientific Services Program, 1307 West Remuda Way, Payson, AZ 85541

US Army Tank-Automotive Research Development and Engineering Center, Warren, MI 48397

## **Abstract**

Lord Rayleigh derived the degree of polarization for singular molecular scattering phenomena in the atmosphere as a function of the relative angular orientations of the source, scattering center and observer. This paper extends the Rayleigh model by giving the azimuth angle for the linearly polarized scattered irradiation detected by the observer. Together these two parameters give a complete Stokes vector characterization of Rayleigh scattering in the earth-horizon coordinate system. An experimental validation confirms the analytical results. The validation methodology uses a polarization axis finder attached to a COTS (commercial-off-the-shelf) digital camera. Each image supplies enough information to calculate the skylight polarization azimuth angle in real time. The equation for the skylight polarization azimuth angle is used to create a pictorial representation of the polarized sky by using colors to represent azimuth angles. A color scheme is used to display the degree of polarization and the polarization azimuth angle of a vehicle at several different times in daylight. An analysis of the reflected polarized light from the vehicle is included.

## **Key Words:**

polarization, polarimetry, visual polarization, digital imaging, image acquisition/recording, image processing

Report Documentation Page			Form Approved OMB No. 0704-0188		
Public reporting burden for the collection of information is estimated to average 1 hour per response, including the time for reviewing instructions, searching existing data sources, gathering and maintaining the data needed, and completing and reviewing the collection of information. Send comments regarding this burden estimate or any other aspect of this collection of information, including suggestions for reducing this burden, to Washington Headquarters Services, Directorate for Information Operations and Reports, 1215 Jefferson Davis Highway, Suite 1204, Arlington VA 22202-4302. Respondents should be aware that notwithstanding any other provision of law, no person shall be subject to a penalty for failing to comply with a collection of information if it does not display a currently valid OMB control number.					
1. REPORT DATE <b>24 JUL 2004</b>		2. REPORT TYPE <b>Technical Report</b>		3. DATES COVERED <b>14-03-2004 to 18-05-2004</b>	
4. TITLE AND SUBTITLE <b>The Polarization Azimuth Angle in Daylight Scenes</b>			5a. CONTRACT NUMBER		
			5b. GRANT NUMBER		
			5c. PROGRAM ELEMENT NUMBER		
6. AUTHOR(S) <b>Roy Matchko; Grant Gerhart</b>			5d. PROJECT NUMBER		
			5e. TASK NUMBER		
			5f. WORK UNIT NUMBER		
7. PERFORMING ORGANIZATION NAME(S) AND ADDRESS(ES) <b>Battelle Scientific Services Program,,1307 West Remuda Way,,Payson,,AZ,85541</b>			8. PERFORMING ORGANIZATION REPORT NUMBER <b>; #14194</b>		
9. SPONSORING/MONITORING AGENCY NAME(S) AND ADDRESS(ES) <b>U.S. Army TARDEC, 6501 East Eleven Mile Rd, Warren, Mi, 48397-5000</b>			10. SPONSOR/MONITOR'S ACRONYM(S) <b>TARDEC</b>		
			11. SPONSOR/MONITOR'S REPORT NUMBER(S) <b>#14194</b>		
12. DISTRIBUTION/AVAILABILITY STATEMENT <b>Approved for public release; distribution unlimited</b>					
13. SUPPLEMENTARY NOTES					
14. ABSTRACT <b>Lord Rayleigh derived the degree of polarization for singular molecular scattering phenomena in the atmosphere as a function of the relative angular orientations of the source, scattering center and observer. This paper extends the Rayleigh model by giving the azimuth angle for the linearly polarized scattered irradiation detected by the observer. Together these two parameters give a complete Stokes vector characterization of Rayleigh scattering in the earth-horizon coordinate system. An experimental validation confirms the analytical results. The validation methodology uses a polarization axis finder attached to a COTS (commercial-off-the-shelf) digital camera. Each image supplies enough information to calculate the skylight polarization azimuth angle in real time. The equation for the skylight polarization azimuth angle is used to create a pictorial representation of the polarized sky by using colors to represent azimuth angles. A color scheme is used to display the degree of polarization and the polarization azimuth angle of a vehicle at several different times in daylight. An analysis of the reflected polarized light from the vehicle is included.</b>					
15. SUBJECT TERMS <b>polarization, polarimetry, visual polarization, digital imaging, image acquisition/recording, image processing</b>					
16. SECURITY CLASSIFICATION OF:			17. LIMITATION OF ABSTRACT <b>Public Release</b>	18. NUMBER OF PAGES <b>31</b>	19a. NAME OF RESPONSIBLE PERSON
a. REPORT <b>unclassified</b>	b. ABSTRACT <b>unclassified</b>	c. THIS PAGE <b>unclassified</b>			



$$\cos \psi = \frac{\sin \alpha \cos \theta - \sin \theta \cos \alpha \cos(\varphi - A)}{\pm \sqrt{1 - (\sin \alpha \sin \theta + \cos \theta \cos \alpha \cos(\varphi - A))^2}} \quad (4)$$

Equation (4) does not include interactions between the incident solar radiation and large atmospheric particles (cloud droplets, ice crystals, aerosols, etc.) and effects due to multiple scattering and molecular anisotropy.

### Validation Methods

Figure 4 is part of an extensive experimental validation study confirming the accuracy of Eq. 4. The experimental apparatus consists of a polarization axis finder<sup>7</sup> attached to a digital camera. The polarization axis finder is a linear polarization element with its transmission axes tangent to concentric circles radiating from its center, as shown in Fig. 5. It attenuates the radiation into two wedge-shaped regions which are aligned parallel to the polarity of the incident linearly polarized light. Figure 4 shows the superposition of a circular protractor with its center coincident with the center of the wedge image. A line through the protractor corresponds to the  $\psi$ -value obtained from Eq. (4) for the appropriate time of day. This line should pass through the center of the wedge-pattern formed by the polarization axis finder confirming the theoretical predictions of our model relating to Eq. 4. Several quantitative methods can be used to validate Eq. (4). One method completely eliminates the need for using the Stokes parameters. Using Matlab<sup>8</sup>, the x-coordinate of the minimum value along each row (y-coordinate) of pixels can be calculated for the wedge region. The slope of the best-fit linear equation for these minimum values corresponds to the polarization azimuth angle. A more exact method for determining the accuracy of Eq. (4) uses the Stokes parameters calculated from the axis finder data.

### Calculating the Stokes Parameters from Axis Finder Data.

The four Stokes parameters,  $S_0$ ,  $S_1$ ,  $S_2$  and  $S_3$  for completely polarized light propagating along the +z-axis are<sup>9</sup>

$$S_0 = E_{0X}^2 + E_{0Y}^2 \quad S_1 = E_{0X}^2 - E_{0Y}^2 \quad S_2 = 2 E_{0X} E_{0Y} \cos \delta \quad S_3 = 2 E_{0X} E_{0Y} \sin \delta \quad (5)$$

where  $E_{0X}$  and  $E_{0Y}$  are the instantaneous amplitudes of the two orthogonal components of the electric field vector and  $\delta$  is their phase difference. The polarization azimuth angle ( $\psi$ ) is determined from<sup>10</sup>

$$\tan 2\psi = \frac{S_2}{S_1} \quad (6)$$

It will be shown shortly that three of the Stokes parameters ( $S_0$ ,  $S_1$ ,  $S_2$ ) are required to determine  $\psi$ , even if the light is elliptically polarized.

If light is transmitted through a linear polarizer with its transmission axis oriented at an angle  $\theta$  with respect to the x-axis, the intensity of the transmitted light can be expressed as

$$I(\theta) = \frac{1}{2} (S_0 + \cos 2\theta S_1 + \sin 2\theta S_2) \quad (7)$$

$I(\theta)$  denotes an intensity measurement corresponding to a particular value of  $\theta$ . Substituting the angles  $0^\circ$ ,  $45^\circ$  and  $90^\circ$  for  $\theta$  into Eq. (7) confers that

$$S_0 = I(0) + I(90) \quad S_1 = I(0) - I(90) \quad S_2 = 2 I(45) - S_0 \quad (8)$$

Figure 6 shows how Eq. (8) can be used in conjunction with a polarization axis finder to determine the Stokes parameters  $S_0$ ,  $S_1$  and  $S_2$ . The transmission axes of the axis finder are circular and tangents to them give the orientation of an infinitesimal linear polarizer. All points along the line between A and A\* in Fig. 6 correspond to linear polarizers with  $\theta = 0^\circ$ . All points along the line between B and B\* and C and C\* correspond to linear polarizers with  $\theta = 45^\circ$  and  $\theta = 90^\circ$  respectively. Figure 7 shows the result of this methodology. The triangular markers on this graph correspond to the average skylight polarization azimuth angle obtained from the axis finder, using the Stokes parameters. They are all nearly coincident with circular markers which were obtained from Eq. (4). Similar results from a multitude of different viewing directions result in the conclusion that Eq. (4) is an excellent tool in predicting skylight polarization azimuth angles.

The circular field of view of the axis finder was measured to be  $10.2^\circ$  and the corresponding circular image had a radius of 480 pixels. However, a cropped circle of radius 140 pixels was used to calculate the skylight polarization azimuth angle. This reduction in the original field of view to  $3^\circ$  produces a very narrow range of skylight  $\psi$ -values and improves the accuracy of the validation methodology.

### **Visualizing the Skylight Azimuth Angle**

In previous work<sup>11-12</sup>, we describe how the Stokes parameters can easily be encoded in a daylight scene. We assign RGB pixel values to the normalized values of  $S_1$ ,  $S_2$  and  $S_3$  at each pixel site in the scene as follows:

$$R = \text{int}[127.5 (1 - S_1)] \quad G = \text{int}[127.5 (1 - S_2)] \quad B = \text{int}[127.5 (1 - S_3)] \quad (9)$$

The pseudo-color scheme described in that work closely relates to the Poincaré representation of polarized light. The equator of the Poincaré sphere plays a very special role in our pseudo-coloring scheme. It corresponds to linearly polarized light ( $S_3 = 0$ ) and is also used to encode the polarization azimuth and ellipticity angles in a daylight scene, as given in Eq. (10). Substituting  $\chi$  for  $\psi$  in Eq. (10) produces a color-mapping scheme for the  $\chi$ -images as given in Eq. (11).

$$R = \text{int}[127.5 (1 - \cos 2\psi)] \quad G = \text{int}[127.5 (1 - \sin 2\psi)] \quad B = 127 \quad (10)$$

$$R = \text{int}[127.5 (1 - \cos 2\chi)] \quad G = \text{int}[127.5 (1 - \sin 2\chi)] \quad B = 127 \quad (11)$$

The degree of polarization,  $P$ , varies between 0 and 1. The simplest method of encoding this parameter in a daylight scene is to use the equation

$$[R,G,B] = 255 P \quad (12)$$

A pictorial representation of a semi-hemispherical region of the celestial sphere, as shown in Figures 8d, 8e, 8f and 8j, 8k and 8l, was created in an Excel spreadsheet. Matlab scripts that incorporate Eqs. (2, 3 and 12) for the  $P$ -parameter and Eqs. (4 and 10) for the  $\psi$ -parameter were written to colorize the areas between the grid lines. The pseudo-colored images relate to clear skies on April 26, 2000 at north latitude 42.5 degrees and west longitude 83.0 degrees. The skylight polarization

parameters are encoded into the drawings as they would appear looking toward the earth, as from a satellite above the earth.

### **The Azimuth Angle in a Daylight Scene**

The vehicle images in Fig. 8 were acquired using an Epson 850Z digital camera. In previous work<sup>12</sup> we described a methodology to obtain the four Stokes parameters for each scene pixel using a COTS digital camera. In this paper we present some applications of these tools and techniques to the analysis of the polarization azimuth angle ( $\psi$ ) for daylight illuminated scenes. Since  $\psi$  depends on the first three Stokes parameters, the analysis is independent of  $S_3$  and consequently wavelength independent. Many factors are important to characterize polarization phenomena for the imagery in Fig. 8 including the ambient light sources, material properties of the scene objects, and relative orientation of the camera, the object and the light source.

Daylight scenes contain unpolarized, broad band sunlight, partially polarized skylight, and indirect diffuse reflection from the ground. The polarization characteristics of these three sources are quite different. Direct solar illumination is nearly collimated and originates from a localized source. Skylight illumination is a distributed source where maximum P originates from a great circle 90° from the sun. The ground plane reflection is very unpolarized and in nearly all cases decreases the average P for the illumination incident on the vehicle surface.

The optical axis of the camera used to obtain Fig. 8 points toward the north, and it is horizontal to the ground plane. The normal to the vehicle vertical panels facing the camera points south. The



vehicle surface is diffuse and reflects incident light into a very large solid angle toward the camera. The specular reflection from sunlight off these panels is primarily directed into the ground plane. Since the sky is a distributed source, light originating from the southern horizon can enter the camera from specular reflection off of the vertical panels. All other reflected illumination entering the camera from the vehicle must be due to diffuse reflections.

Equation 13 predicts<sup>13,14</sup> that the angle of incidence for sunlight incident on the vehicle is given by the following expression:

$$\cos i = \sin z \sin A \sin s \sin \gamma + \sin z \cos A \sin s \cos \gamma + \cos z \cos s \quad (13)$$

where  $i$  = angle of incidence,  $z$  = zenith angle of sun,  $A$  = azimuth angle of sun,  $s$  = slope of plane surface and  $\gamma$  = azimuth angle of plane surface. The azimuth of the plane is measured westward from south and is zero when the normal to the plane points toward the south. Equation 13 is derived from the vector dot product of a unit vector  $\mathbf{R}$  towards the sun and a unit vector  $\mathbf{n}$  normal to a plane surface. Analysis of Fig. 9 shows that

$$\mathbf{R} = \sin z \sin A \mathbf{i} + \sin z \cos A \mathbf{j} + \cos z \mathbf{k} \quad (14)$$

$$\mathbf{n} = \sin s \sin \gamma \mathbf{i} + \sin s \cos \gamma \mathbf{j} + \cos s \mathbf{k} \quad (15)$$

At 07:00 the sun is near the eastern horizon with  $\alpha = 3.8$  and  $A = 254.9$  degrees. Thus skylight is highly polarized near the meridian, opposite the side of the vehicle facing the camera, which is shown in Fig. 8d. Also, the skylight  $\psi$ -value along the horizon is approximately 90 degrees (see Fig.

2a). Since the sun is located in the northeastern quadrant of the sky, no direct solar irradiation is incident on the panels facing the camera since the vehicle is positioned parallel to an east-west direction.

Figures 8a and 8g show that paint color affects the polarization state of the reflected light. A good example of this phenomenon is the door panel, which has two distinct paint colors. The reflected light from those regions have different values for  $P$  and  $\psi$ . The  $\psi$  angles are approximately 60 and 90 degrees for the two regions.

At 19:00 the sun is near the western horizon in the northwestern quadrant of the sky with  $\alpha = 14.8$  and  $A = 95.4$  degrees. Similar to the previous case, no direct solar radiation is incident on the southern panels. Since the relative positions of the sun, vehicle and camera are nearly symmetrical with respect to the N-S direction at 19:00 compared to 07:00, the  $P$  and  $\psi$  images at these two times are very similar. Figure 8 also shows that the azimuth angle of the reflected light from the vehicle panels is approximately equal to the skylight azimuth angles near the meridian and the horizon, i.e. in the direction of the digital camera.

Figure 10 shows the laboratory experiment used to obtain the Stokes parameters from vertical panels. These studies indicate that diffuse reflections originating from incident polarized light produce azimuth angles that vary for different pigments. One of the pigments showed that diffuse reflections have reflection azimuth angles that are the mirror images of the azimuth angles of the incident light. This phenomenon was observed for the following conditions: (1) viewing along the normal to the vertical panel, (2) polarized incident light, and (3) all incident and azimuth angle

configurations for the linearly polarized light source. This behavior is clearly seen in Fig. 11 and the daylight scenes in Fig. 8. This data also shows that the P-value (Fig. 12) is very dependent upon the azimuth angle of the incident light for angles of incidence near 90 degrees.

An interesting relationship exists between the polarization azimuth angles produced by sunlight reflected off of vertical vehicle panels, and the azimuth angles of the incident skylight oriented along the meridian and on the horizon. These angles are equal as shown in the next paragraph.

If  $\mathbf{r}$  is a unit vector  $180^\circ$  with respect to an incident sun ray, then

$$\mathbf{r} = \sin z \sin A \mathbf{i} + \sin z \cos A \mathbf{j} + \cos z \mathbf{k} \quad (16)$$

Let  $\mathbf{n}$  be a unit vector parallel to the surface normal of a vehicle panel. Then,  $\mathbf{n} = \mathbf{j}$  and the vector cross product produces

$$\mathbf{R} = \mathbf{r} \times \mathbf{n} = -\sin \alpha \mathbf{i} + \cos \alpha \sin A \mathbf{k} \quad (17)$$

The geometry in Fig. 13 shows that

$$\cos \beta = \frac{\sin \alpha}{\sqrt{1 - \cos^2 \alpha \cos^2 A}} \quad (18)$$

The polarization azimuth angle is obtained from  $\psi = 180 - \beta$ .

Using the 12:00 sun position in Eq. (18) produces a reflected solar  $\psi$ -value of 155.7 degrees.

Inserting  $\phi = 0$  and  $A = 0$  into Eq. (4) yields

$$\cos \psi = \frac{\sin \alpha}{\sqrt{1 - \cos^2 \alpha \cos^2 A}} \quad (19)$$

Equation (19) gives the skylight  $\psi$ -value, as seen from the earth, of a point on the meridian ( $A = 0$ ) and on the horizon ( $\phi = 0$ ). Skylight traveling from this point toward a vertical panel on the vehicle propagates along the normal to the panel. It reflects off the panel as a mirror image of the incident skylight. The camera records a  $\psi$ -value that is the supplement of the value obtained from Eq. (19), namely 155.7 degrees at 12:00. According to the color key for  $\psi$ -values in Fig. 8, this  $\psi$ -value corresponds to a medium green color. This is the color seen in Fig. 8h for vertical panels with a surface normal toward the south. The Stokes parameters for reflected light from the vehicle panels (averaged over 10 X 10 pixel areas) also gives  $\psi$ -values near 150 degrees.

Temporal registration errors, originating from the 30 second data acquisition period of the Epson 850Z, are not significant in obtaining valid  $\psi$  values. The change in luminance due to solar radiation and skylight during the 30 second data acquisition period also has little effect on the Stokes parameters for these targets.

### **The Degree of Polarization in a Daylight Scene**

Figures 8a and 8c at 07:00 and 19:00 show much less contrast and higher P-values than the imagery at 12:00. Figures 8d and 8f at 07:00 and 19:00 show that highly polarized skylight exists at all altitudes in the southern sky, i.e., along the meridian and directly opposite the vehicle. Figure 14 shows that both edges and vertical panels can reflect highly polarized light into the camera. Since P is large for both of these regions, there is little contrast between them in the imagery. Since the sun is behind the vertical plane at 07:00 and 19:00, direct sunlight can not contribute to producing polarized reflected light from the vehicle. At 12:00, the altitude and azimuth of the sun are 55° and

319° respectfully. Highly polarized skylight, visible to the panels, is near the eastern and western portions of the sky; hence, its contribution to the degree of polarization of reflected light from vertical panels along the optical axis of the camera is much less than at 07:00 and 19:00.

As Fig. 15 illustrates, only solar specular reflections from rounded edges can enter the camera at 12:00 while specular reflections from vertical panels are directed into the ground plane and not visible to the camera. However, sunlight that reflects diffusely from both edges and vertical panels can be seen by the camera. Laboratory studies<sup>15</sup> show that the highest degree of polarization (0.55) occurs for obtuse angles between the incident unpolarized light and the light reflected from the surface. Since obtuse diffuse reflection angles are directed into the ground plane, edges will show a larger degree of polarization than vertical panels. This phenomena explains why there is more contrast between the vertical panels and edges of the vehicle in the 12:00 P-image.

## **Conclusions**

This paper gives a complete description of linearly polarized light originating from single molecular scattering mechanisms. Since there is no elliptical polarization<sup>5</sup> from primary Rayleigh scattering, the Stokes vector for this case contains two independent components: the degree of polarization first derived by Lord Rayleigh, and the azimuth angle described in this paper. Both of these parameters are written with respect to an earth-horizon coordinate system. The latter is convenient for predicting polarization effects due to solar illumination in planetary atmospheres. Both parameters are dependent upon the relative orientation of the illumination source, scattering centers and observer. The degree of polarization is important for determining the presence of linearly polarized

light in daylight scenes. The azimuth angle is particularly important for determining the orientation and curvature of secondary scattering surfaces that are illuminated by direct sunlight and indirect polarized skylight.

Temporal registration errors caused by 30 second time delays in the image acquisition process do not appear to be important for obtaining accurate  $\psi$ -values in solar illuminated imagery. The small variations in solar luminance during the data acquisition period also have little effect on the accuracy of Stokes parameter measurements for these scenes.

## References

1. Astronomie Populaire, 2; 99.
2. *Phil. Mag.*, **41**: 107, 1871.
3. M. Born and E. Wolf, *Principles of Optics*, 6<sup>th</sup> ed., (Pergamon Press, New York, 1993), pp. 652-656.
4. W. J. Humphreys, *Physics of the Air*, (Dover Publications 1964), p. 561.
5. K. L. Coulson, *Polarization and Intensity of Light in the Atmosphere*, (Deepak Pub., Hampton, VA, 1988), p. 177.
6. F. A. Jenkins and H. E. White, *Fundamentals of Optics*, 3<sup>rd</sup> ed., (McGraw Hill, New York, 1957), pp. 505-507.
7. Thermo Oriel, 150 Long Beach Blvd., Stratford, CT 06615.
8. The Math Works Inc., *MatLab*, 24 Prime Parkway, Natick, MA 01760.
9. M. Born and E. Wolf, *Principles of Optics*, 6<sup>th</sup> ed., (Pergamon Press, New York, 1993), p. 30.
10. M. Born and E. Wolf, *Principles of Optics*, 6<sup>th</sup> ed., (Pergamon Press, New York, 1993), pp. 554-555.
11. G. R. Gerhart and R.M. Matchko, "Encoding Polarization Parameters in a Daylight Scene," Proceedings of the Ground Target Modeling and Validation Conference, August 2002.
12. R. Matchko and G. Gerhart, "Polarization Measurements Using a COTS Digital Camera", included for review
13. R. Matchko and G. Gerhart, "Luminance, Contrast and Polarization of White Light Reflected from Ground Combat Vehicles", ADA265255, TACOM Research Development and Engineering Center, Warren, MI (1992), Appendix D, pp. 301-302.

14. R. Matchko and G. Gerhart, "Reflection and Polarization of White Light from Ground Vehicles", ADB271426, TACOM Research Development and Engineering Center, Warren, MI (1998), Appendix B, pp. 385-386.
15. Ibid., pp.288-295.



## Figure Captions

**Figure 1.** The observation plane PAO containing an incident solar ray PA, a scattering center P, the observer O and the scattering angle  $\Omega$ .

**Figure 2.** Scattered waves that produce linearly polarized skylight with polar axes arranged in concentric circles about the direction of propagation.

**Figure 3.** The geometry for finding the polarization azimuth angle for primary Rayleigh scattering.

**Figure 4.** Polarization of skylight at 07:31 on Sept. 7, 2001 at Payson, AZ (long. = 111.35° W, lat. 34.23° N);  $\alpha = 17.3^\circ$ ,  $A = 274.8^\circ$ ,  $\theta = 20^\circ$ ,  $\phi = 0^\circ$ . Equation 4 predicts that  $\psi = 75.2^\circ$ .

**Figure 5.** A polarization axis finder is a linear polarization element with its transmission axes tangent to concentric circles radiating from its center.

**Figure 6.** The geometry of a polarization axis finder used to obtain the Stokes parameters.

**Figure 7.** Comparison of skylight polarization azimuth angles. Values marked with circles are obtained from Eq. (4). Experimental values that are obtained from the axis finder are marked with triangles.

**Figure 8.** The images above relate to clear skies on April 26, 2000 at north latitude 42.5 degrees and west longitude 83.0 degrees. A normal to a vertical vehicle panel, which faces the digital camera, points south; the camera view is toward the north. The skylight drawings are pictorial representations of the polarized sky in the southern semi-hemispherical region of the celestial sphere. The skylight polarization parameters are encoded into the drawings as they would appear looking toward the earth, as from a satellite above the earth. The degree of polarization (P) is encoded into the scenes using  $[\text{pixel value}] = 255 P$ . The polarization azimuth angle ( $\psi$ ) is encoded into the

scenes using RGB pixel values corresponding to  $R = \text{int}[127.5 (1 - \cos 2\psi)]$ ,  $G = \text{int}[127.5 (1 - \sin 2\psi)]$  and  $B = 127$ . Skylight  $\psi$ -values were obtained from Eq. (4).

**Figure 9.** Geometry for deriving the angle of solar incidence.  $\mathbf{R}$  is a unit vector towards the sun and  $\mathbf{n}$  is a unit vector normal to a surface.

**Figure 10.** In-house experimental setup to obtain the Stokes parameter for reflected light from a vertical panel.

**Figure 11.** Reflected  $\psi$ -values obtained from the in-house experiment shown in Figure 10.  $\beta$  is the azimuth angle of the incident light.

**Figure 12.** Reflected P-values obtained from the in-house experiment shown in Figure 10.  $\beta$  is the azimuth angle of the incident light.

**Figure 13.** Geometry for finding  $\psi$ .  $\psi = 180 - \beta$ .

**Figure 14.** At 07:00 and 19:00, highly polarized skylight along the meridian is incident on the target.

**Figure 15.** At 12:00, only specular reflections of sunlight from edges can enter the camera; specular reflections from vertical panels are toward the ground.

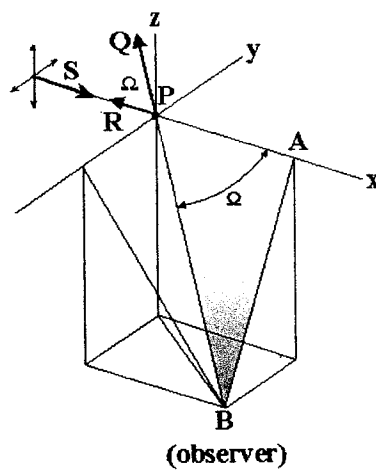


Figure 1

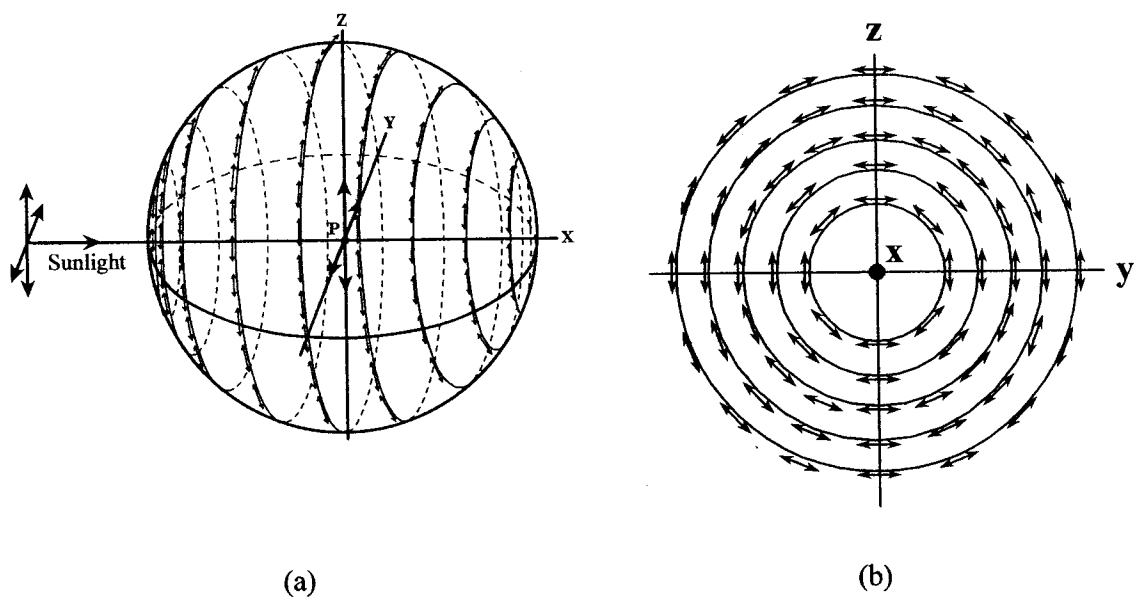


Figure 2

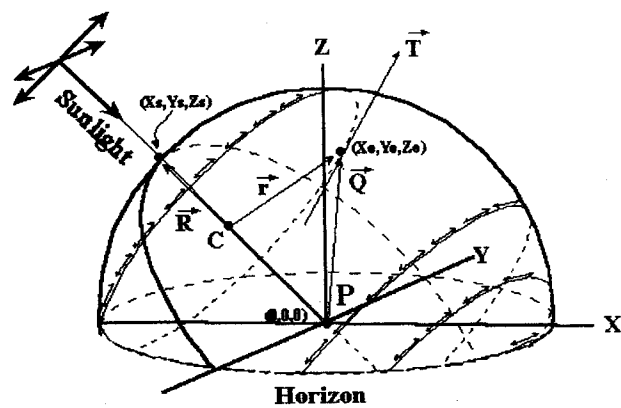


Figure 3

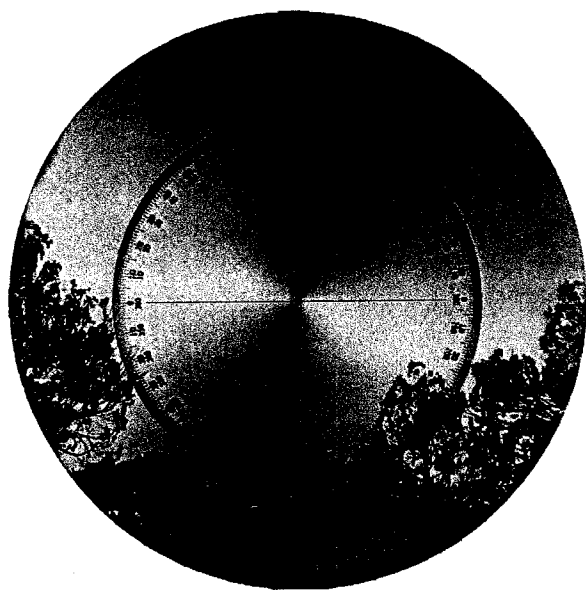


Figure 4

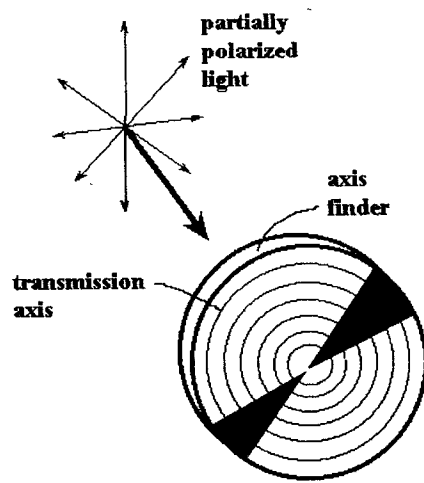


Figure 5

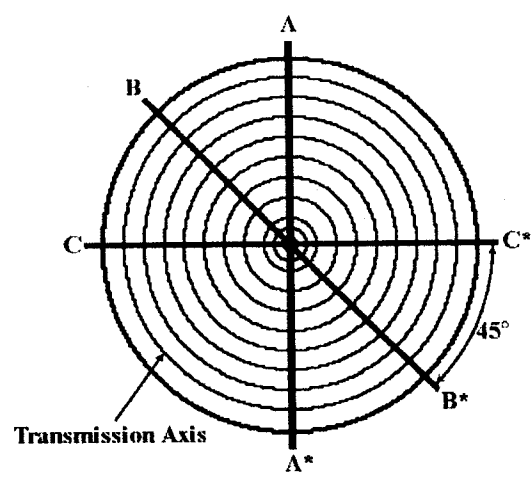


Figure 6



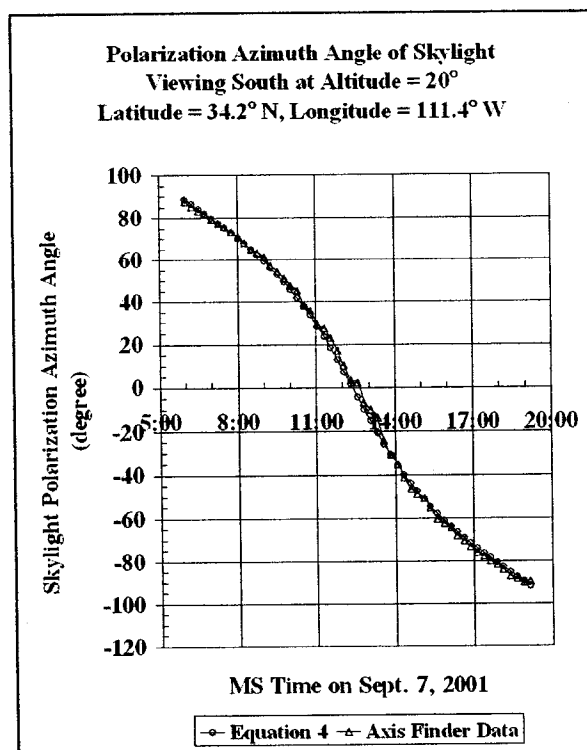
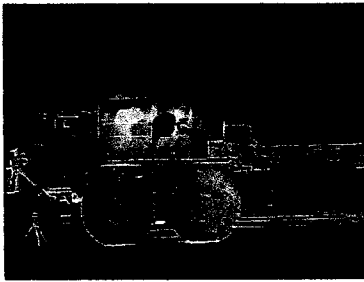


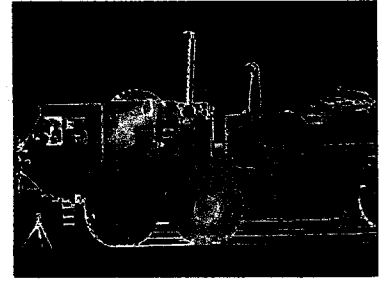
Figure 7



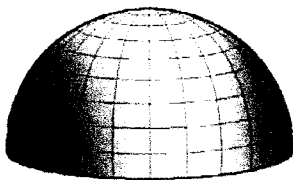
(a) P of Vehicle at 07:00



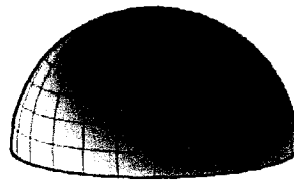
(b) P of Vehicle at 12:00



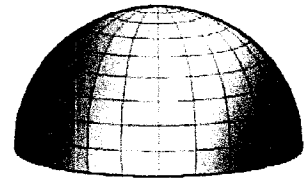
(c) P of Vehicle at 19:00



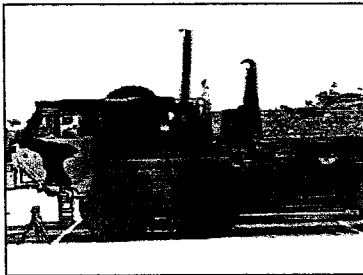
(d) P of Skylight at 07:00



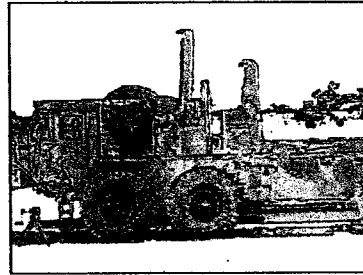
(e) P of Skylight at 12:00



(f) P of Skylight at 19:00



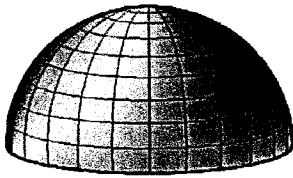
(g)  $\psi$  of Vehicle at 07:00



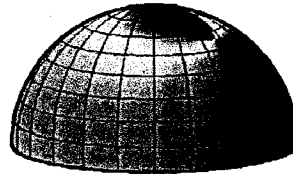
(h)  $\psi$  of Vehicle at 12:00



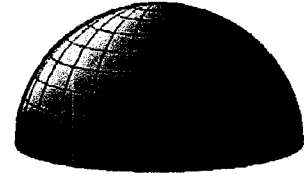
(i)  $\psi$  of Vehicle at 19:00



(j)  $\psi$  of Skylight at 07:00



(k)  $\psi$  of Skylight at 12:00



(l)  $\psi$  of Skylight at 19:00

Color key for  $\psi$ -values:



Figure 8

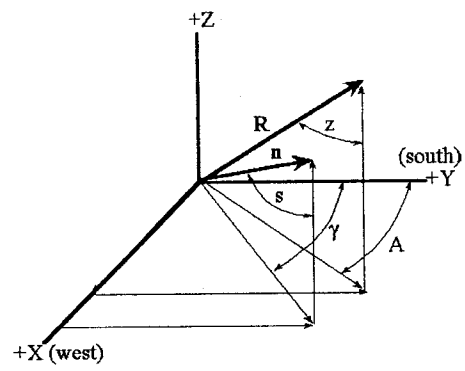


Figure 9

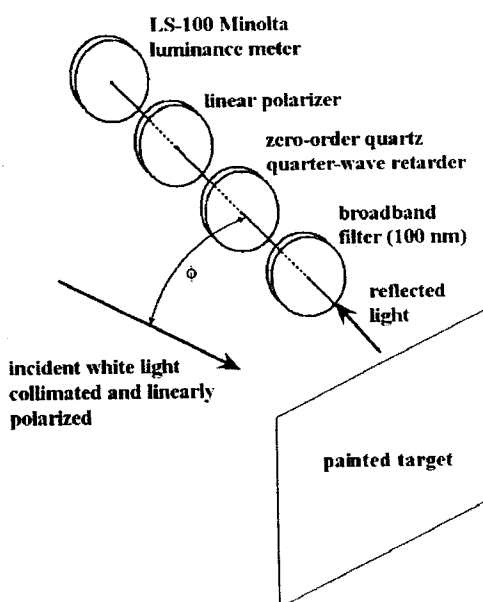


Figure 10

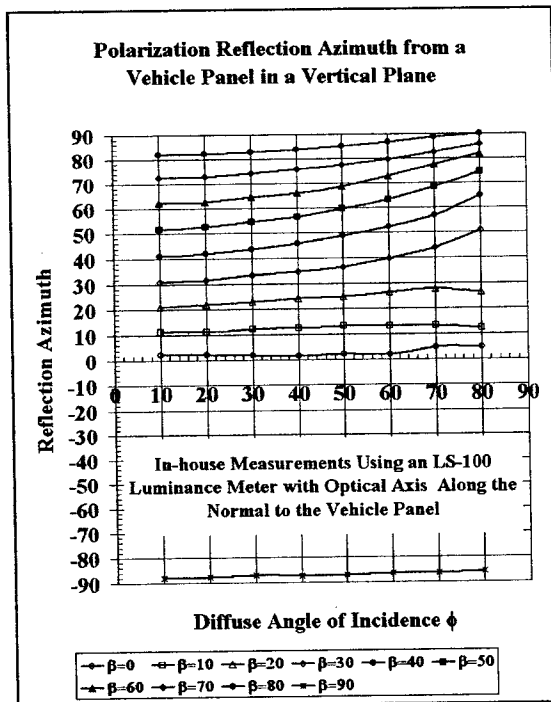


Figure 11

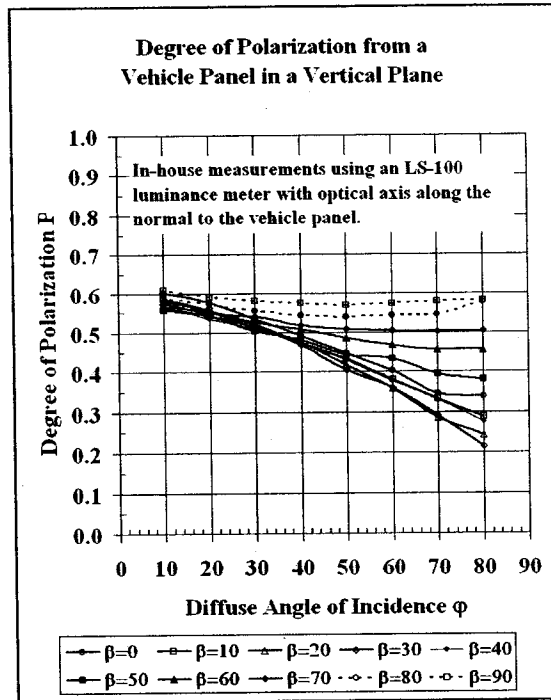


Figure 12

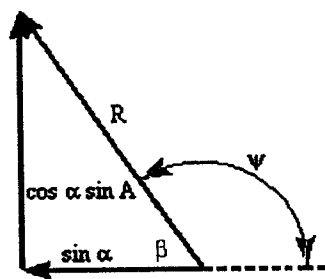


Figure 13

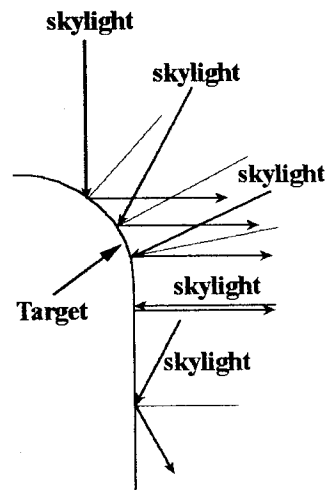


Figure 14



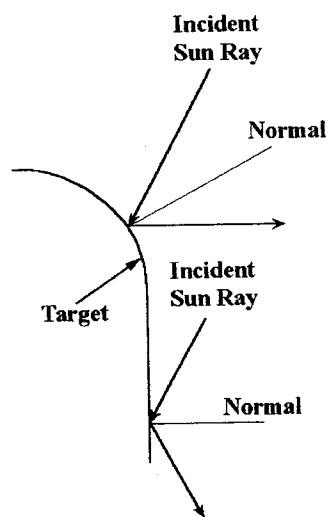


Figure 15